Calibrated Digital Imaging Systems *

by Vladimir Tamari and Masato Kobori

Tokyo, April 1982

The concept of simulating chosen information channels of a linear incoherent imaging system by projecting reference signals is proposed and the system's ability to restore severely distorted but stationary images is experimentally demonstrated. A particular instrument's object field is divided into N discrete 'points' whose individual simulated outputs is measured at N particular sampling points; the NxN output matrix F is the transfer matrix of the system, and being empirically derived, it precisely accounts for all diffractions, aberrations, distortions, peculiarities of the chosen object points and sensor size and distribution. As such F can become the basis for eliminating algorithm-hardware mismatch in various restoration schemes. Calibration allows treating the instrument as an unknown 'black box', and imaging through a severely and arbitrarily distorting hardware is demonstrated. Other uses of F are to add or subtract the outputs of separate instruments viewing the same object on a pixel-by-pixel basis, and as a graphically or digitally presented measure of the instrument's local transfer function, and hence of image quality.

I. INTRODUCTION

Imaging instruments have been described by Toraldo di Francia[1], Frieden[2], and others, as input-output systems utilizing information-carrying channels [3] to transmit signals from an object to an image. We use this concept to propose adding a simple empirical step to a particular linear, incoherent time-invariant imaging system: N randomly chosen band- limited spatial â€˜points' in the object field are simulated by known reference signals, one point at a time. The point-spread function (PSF) of each object point is partially sampled by one or more of N particular sensors in the image field. The sensor response functions (SRF) for the N object points then become an empirically-derived NxN F matrix completely defining, within the measurement noise limitations, the instrument's channel capacity between the chosen objects and the sampling points of such an image. As such, F contains, quantized *a priori* information, accounting for the instrument's diffractions, aberrations, distortions, edge effects, as well as for the extent of the object field and point size and distributions. Variations and irregularities of sensor size and distribution or sensitivity and cross-talk (if the effect is linear) will also be accounted for in F. F can have several uses in the following areas:

1) Optimizing known restoration schemes by providing the actually sampled PSF value rather than the idealized sinc function which only applies to the isoplanatic region[4] of diffraction-limited hardware when they are perfectly sampled by ideal sensors. F can provide accurate mapping of useful portions of an image field, saving computational effort outside this portion.

2) Imaging through unknown hardware that can have a severely unfocused, distorted or uncharacterized PSF, as in crystals, or through stationary aberrated systems, when knowledge of F allows a coarse but distortion-free restoration. This function is demonstrated experimentally in section VII of this paper.

3) Absolute pixel-to-pixel addition or subtraction of the digital outputs of two or more separate instruments imaging the same object. Calibration provides the exact knowledge of the object field points, so that even if the instruments have different distortions, magnifications, and aberrations, the outputs can still be combined, either as direct images, or as restored objects.

4) The data in F provides a ready reference of image quality in a particular portion of the image field. Graphically presented as a chart of gray levels, F is generally a band matrix that is â€˜thinnest' at the point of best focus. More quantitative analysis of F will provide a numerical value, of the local image quality such as the conditioning number[5].

In this paper, we consider a spatial object domain. Calibration can also be performed in the frequency domain, where each object 'point' becomes a particular sinosoidal input across the whole object field. Other possibilities are to calibrate the color, polarization or other object signal qualities that will affect the image of a particular instrument. For simplicity, such schemes will not be treated here, except to say that the F matrix in such cases will be of size (NxNxMxL...) where M,L... are the various discretized object qualities being considered. Calibrated Digital Imaging Systems (CDIS) provide a general tool applicable to any linear incoherent system, but we have stressed the optical approach.

II. THE F MATRIX

The concept of the impulse response of a system appears in many guises. As Green's theorem [6], it is the basis for integration by parts. In control engineering [7] it is a practice to apply reference signals as inputs of closed-loop servomechanisms, and to study the response. As the Dirac Delta Function [8]he impulse function is a useful mathematical tool in optical derivations because it is based on the physical fact of atomic photon emission. An object function O_i where i=l,2,3...N consists of weighted delta functions, and when N is finite, each discretized object point O_i can be considered the input of one imaging channel. It is not required that the O_i be connected, be distributed regularly, have equal size or shape, as long as these characteristics are invariant. In addition, O_i need not represent the whole image field of a given instrument, or even lie on the same plane. They are chosen because of some particular interest in those regions. The $O_{i.}$ signals pass through a particular hardware of unknown transfer function, and add up linearly in an image plane where at least one sensing point S_j , j=1,2,3...N is necessary to identify signals from any one $O_{i.}$. Again, the size, shape, distribution, or sensitivity of the S_j sensors can be arbitrary as long as these characteristics are invariant. Intuitively, in this special case, a sufficient and necessary sampling rule can be stated as follows: each O_i emits signals received by one or more S_j, and each $S_{j.}$ receives signals from one or more O_i. This guarantees a minimum of one channel between N unique object and sensing point pairs, while superfluous sensing points will be discarded when they do not receive any signal. A computer check can ascertain whether this rule has been followed after the F matrix has been compiled, extra sensing point data is then added or discarded as the case may be. The relationship between the O_i and S_j points is given by the well known discretized imaging equation :

$$S == F.O+n \qquad (1)$$

where S is the sensor data column S_j, O is the object intensity column O_i, and F is an NxN transfer matrix defining the channel capacity between each O_i and S_j, and n is an N-element noise column caused by measurement errors. An element f_{ij} exists for any possible pairing of Oi with Sj, and the difference between the values of f_{ij} and those of a theoretically-derived transfer matrix are easy to see: in CDIS it is the actual channel capacity between a particular and known O_i and a known sensor S_j that is given by the F matrix associated with the instrument at hand. It is this fitting of the matrix data to the actual hardware that gives the method its advantage. Superficially Eq.(1) resembles the imaging equation for other systems, but it must be kept in mind how F was derived. In the case of a diffraction limited optical system, each column of F will consist of a discretized sinc function, but only if all S_j and O_i are equal in size and equally tessalated; it is easy to see that where these assumptions do not hold, the restoration based on the diffraction-limited deconvolution kernel will suffer.

Calibration entails simulating each object point O_i in turn with a signal emitted with intensity C. The SRF associated with any one point O_i is $S_{j\ OiC}$ and is stored as one column of the calibration

matrix F_C. In reality, the completed F_C will consist of the set of *measured* SRF columns associated with each O_i:

$$F_C = F.C + n_C \qquad (2)$$

where F is the instrument's transfer function for unit impulses, and n_C is an NxN matrix consisting of the measured noise during calibration. From Eq.(2):

$$F_C = (F_C - n_C)/ C \qquad (3)$$

Substituting Eq.(3) into Eq.(l), while adding a subscript (I) to the measured noise column of Eq.(l) to distinguish it from the measured calibration noise matrix n_C gives:

$$S = [\, O(F_C - n_C)/ C \,] + n_I \qquad (4)$$

which is the CDIS version of Eq.(l) . The extra noise term n_C is an added burden, especially since it must also include any errors due to faulty simulation procedures, and the 'phasing-errors' to be discussed later. However calibration can be performed under controlled conditions and n_C minimized, for example by averaging several calibrations.

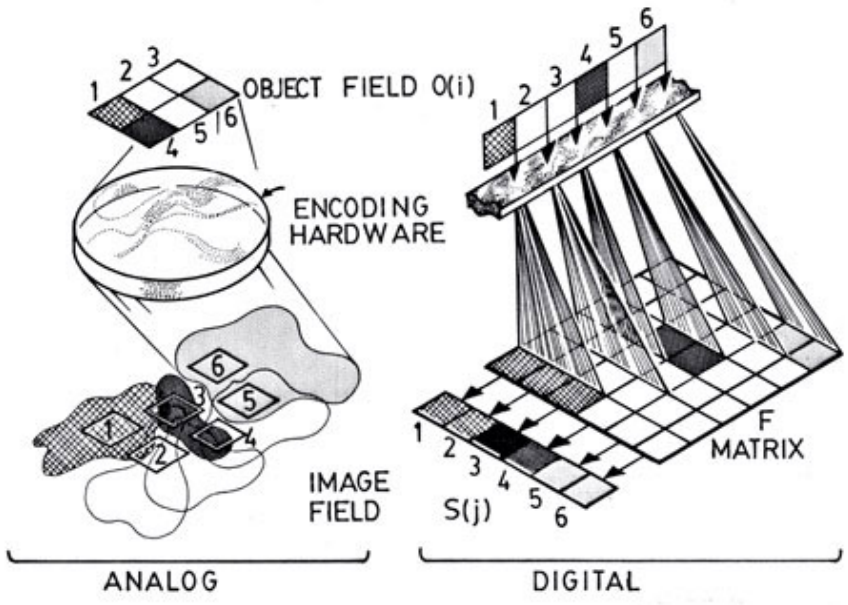

a **b**

FIGURE I An imaging instrument and its calibration matrix. (a, left) Analog imaging situation where object points are imaged by an aberrated lens. The spatial domain object field O_i gives a distorted, overlapping, and irregularly sampled image; (b, right) A conceptual digital representation of (a), where the aberrations are accounted for in the calibration step (not shown here) to obtain the transfer matrix F. Each object O_i contributes a uniquely weighted radiation pattern over various sensors, shown as columns of F. Sensor readings S_j are a result of horizontal summations of the weighted elements of the matrix rows.

Fig.l a.b. illustrates Eq. (l) for a rough optical system; (a) the actual analog situation of a rough imaging lens and (b) as the equivelant mathematical model, where the F matrix is explained conceptually to explain how the data is used. Contributions from the object points O_i are shaded according to the numerical strength of the signal, and in the analog case (a) the overlapping PSFs fall on an irregularly sampled image field. In the digital representation the vertical channels represent multiplication (weighting) of O_i signals into the columns of the F matrix, and each column SRF is the CDIS equivalent of the analog PSF. In the image field, rows of F are added up horizontally, giving the direct summed up image function S_j.

Different solutions for offered Eq. (l) have been offered, and no attempt will be made to list the many algorithms available, but in the following section the effects of using the F matrix on some of these algorithms will be studied.

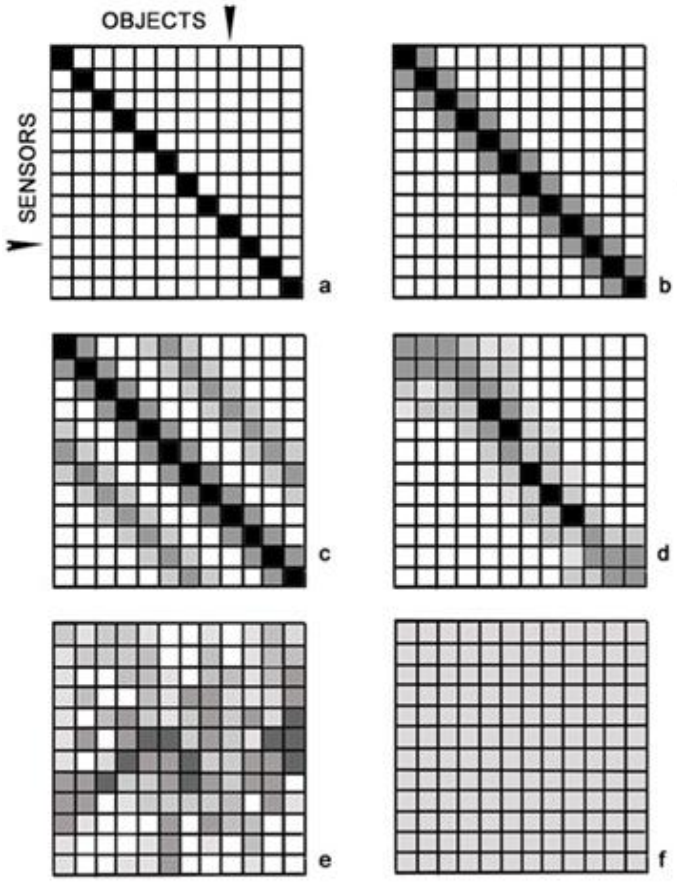

FIGURE 2 Graphic presentation of types of transfer matrices F for various types of focusing, (a) The ideal instrument (b) 1-D diffraction-limited case. (c) 2-D diffraction-limited (bands result from sensor labling strategy), (d) A system with aberrations and distortions, (e) Severe distortion, yet with sufficient autocorrelation peaks to distinguish signals in different columns, (f) Total scattering, or the case of no focusing.

Fig.2 (a-f) shows the F matrices schematically for different types of focusing capabilities. Highest values are shown as black matrix elements, and lower values as different gray levels with white for zero. (a) shows the ideal imaging instrument's F matrix, where each object point is imaged as a unique image point [9], when F becomes a diagonal matrix whose every non-zero element gives the channel transmission capacity. The F matrix of a super-resolving instrument will look like this. (b) shows the isoplanatic patch of a diffraction-limited instrument when the elements of F spread slightly from the diagonal, in the 1-D case, and horizontal rows sum up contribution from the column sine functions. The degree of overlap depends on the finesse of the calibration, i.e. on the object and sensor point size. (c) shows F for the 2-D diffraction-limited case: the number of bands

corresponds to the PSF covering sequentially labeled sensor rows in the image plane of the actual instrument, causing neighboring sensor elements to have discontinuously numbered labels. Each column (and each row, if the PSF is symmetrical) will consist of discretized samples from the total PSF area, as in Lahart's [5] algorithm. (d) shows F for a system, where the PSF changes from point to point: paraxial regions are seen when the data band narrows to a minimum, parallel stripes straddling the diagonal maximum. Distortions are noted if the data band curves away from the diagonal while still being fairly compact, while aberrations cause the data to become splayed, with decreased contrast between the data elements of a column.(e) shows the F matrix for an instrument providing sharp autocorrelation peaks, but whose PSF is quite irregular, causing severe overlapping, as in the case of coded-aperture imaging, or in the case of diffraction from gratings or crystals, or as in the instrument illustrated in Fig 6 below, from an arbitrary screen made up of various lenses. Compare (e) with Fig.7, which plots the SRF of the experimental calibration. (f) shows the F matrix in the extreme case of either total scattering or of the absence of any encoding hardware, when the elements of F become full of overlapping undifferentiated signals, and F becomes singular, and imaging impossible.

III. THE ROLE OF F IN RESTORATION SCHEMES

Frieden, [10] in his review of restoration algorithms refers to the general equivalence of frequency domain and spatial domain treatments. Lahart[5], while concluding the same, points out that Fourier treatment is more fit for global restoration of invariant (stationary) systems, particularly with images assumed to be diffraction-limited with a sinc PSF. Many of the published restoration algorithms such as Phillips' pre-smoothing method [10], Gerchberg's extrapolation [11], Helstrom's least squares [12], and. Mammone and Eichmann's use of linear programming [13] and others, depend on some manipulation of the transfer matrix, which is usually assumed to be the diffraction-limited ideally and continuously sampled image. To fit such 'perfect' algorithms to the images made with instruments that are less than perfect will cause the restoration to suffer. Without calibration, it is very difficult to check if the diffraction-limited requirements have been met, and in the majority of the algorithms mentioned, there is no provision to rectify the procedure if the PSF is found to vary from place to place in the image, or if a faulty sensor element is discovered, causing an algorithm-hardware mismatch. In the Fourier domain the F matrix can be compiled by simulating a set of sinosoidal inputs of varying frequency, in the manner of instruments used to measure the optical transfer function (O.T.F.) [14]. Such empirically derived F matrices will fit the actual hardware used better, with an expected improvement in the restoration. Lahart [5] has described one type of spatial domain pixel-by-pixel restoration, and CDIS methods should prove particularly useful to optimize such restorations by: 1) providing the local SRF value, rather than an idealized deconvolution kernel. 2) Computational effort can be saved by confining the restoration to those portions of F that are known to be well focused. Alternately for aberrated regions, neighboring rows and columns of F can be summed up and the restoration coarsened by increasing the size of the object and sensing 'points' outside paraxial regions, much as the eye's resolution of peripheral regions is less than that of foveal vision. 3) When portions of S_j are zero, the F matrix pinpoints the exactly corresponding zero object points, as in Fig. 3.

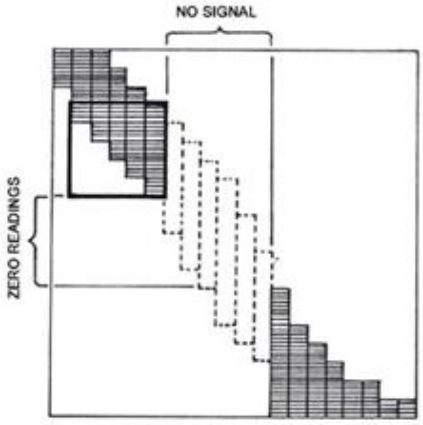

Fig. 3 The F matrix used for restoring signals near a known dark field. The data band is known from calibration, and when a set of sensors give zero readings, the corresponding zero objects will be known, even in non-stationary cases. Sub-matrices (heavy square) can then be used to restore edge signals iteratively.

This permits edge enhancement with a much smaller matrix, and a 'running' iterative restoration away from the edges can be made, substituting restored (solved) object weighting values in each successive set of columns of F.

Fig.4 summarizes the concepts of this section. Hitherto digital imaging is confined to steps 6,7 and 8, (including a theoretically compiled version of 5), when unknown signals enter some instrument and the restoration is made using essentially assumed relationships between the hardware used and the restoration algorithm. By adding the calibration steps 1,2,3,4, the F matrix becomes a hardware-derived set of data on which can be based the restoration algorithm (step 5). The significance of step 4 might not be too obvious at first: it is the a- priori information about simulation source position and size, i.e. the parameters of the object point geometry and field extent, absolute position in space etc. This data is not directly visible in the F matrix, but can be put to good use when the restored data is displayed. Step 4 is analogous to knowledge of X-ray source angular position in medical tomographic imaging. The closed-loop nature of the system in Fig.4 suggests that the calibration mechanism might be made to double as an analog optical processor for performing the restoration by repeated passes, as in the system described by Goodman et al [15] for incoherent optical matrix-vector multiplication, but in that case the process cannot be described as a calibration process, although the same hardware will be in use as for CDIS. The possibility of this application is interesting because the imaging equation Eq.(l) is also a matrix-vector multiplication F.O

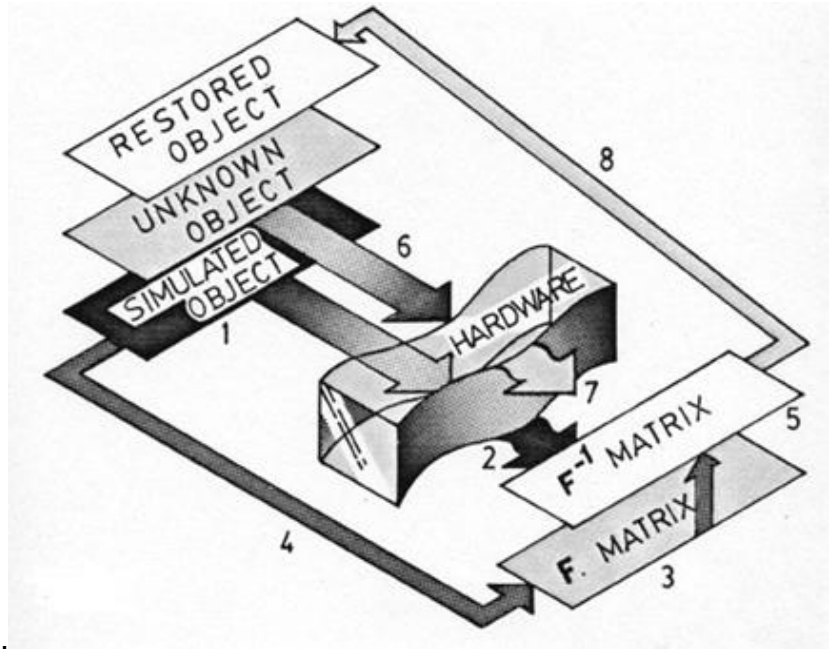

FIGURE 4 Schematic diagram showing the closed-loop feedback nature of CDIS imaging. Point signals 1 are simulated, and the encoded calibration image 2 is recorded as the sampled PSF in one column of F. Steps 3 and. 4 signifies the a priori knowledge of simulated point size, field extent and absolute position in space. A restoration algorithm 5 is then used to restore an unknown signal 6, passing through the same calibrated hardware, 7, and a restored object obtained 8.

IV. THE INVERSE RESTORATION

In most high-resolution applications, F is known to be ill conditioned when a simple inversion of Eq. (4) will be too sensitive to noise. In special cases when rough resolution is acceptable and the F matrix well behaved, the direct inverse restoration can be used, for example in X-ray or nuclear application. From Eq.(4):

$$O_i = F_C^{-1}.S(j) = O(i)\{1 - F_C^{-1}n_C + F_C^{-1}n_I\}/C \qquad (5)$$

Giving the estimate as a ratio of the calibration intensity C, and with the attendant double noise errors already referred to. Discretizing a continuous function gives rise to another source of errors which arise when a strong impulsive signal is smaller in extent than the spatial calibration point size A, as in Fig.5, and the image cannot fit within the corresponding PSF or its sampled SRF

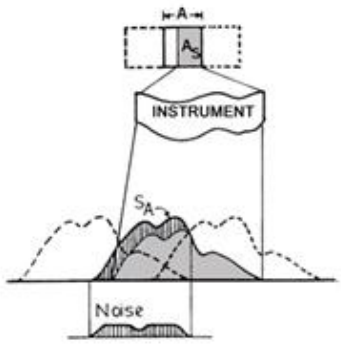

Fig. 5. 'Phasing-Errors' occur when a strong impulsive signal A_s is smaller in size than the calibrated object point size A, resulting in a mismatch between the actual and the calibrated PSF.

If neighboring PSFs have similar shapes, this 'phasing error' is likely to be a horizontal dc term, but in very rough systems, neighboring PSFs will not resemble each other, and the impulsive object's PSF will not resemble any of the calibrated PSFs. Such errors appear in Hadamard spectroscopy, and have been treated by Fenimore and Weston [16] through fine sampling. The Equivalent CDIS treatment would be either to make a new calibration using smaller points and sensors, or to create new rows and columns in F by calculation of the intermediate values. This of course is only possible if there exist extra unused sensors elements that had been left out of F.

V. THE F MATRIX AS A MEASURE OF IMAGE QUALITY

It has been demonstrated in section B. and in Fig.2, how the F matrix, converted into graphical form, can be a quick visual reference mapping of the imaging system's focusing efficiency, in terms of the specific sampling points used for the calibration. This is akin to the "F1F2 Diagram" proposed by Goodman [17], which however is based on the computed cross product of object Fourier transforms.

Another approach, following Lahart [5] is to compute the conditioning number of F, which is a measure of the stability of the system of linear equations represented by Eq.(l) and hence, their susceptibility to noise. The conditioning number will then be a spatial version of the O.T.F. This is not for descriptive purposes only, since an unstable F can be improved by adding neighboring rows and columns until F is better behaved, with a smaller conditioning number. This number is the product of some norm of the matrix with its inverse

$$(F)= ||F||\ ||F^{-}|| \qquad (6)$$

one such norm being:

$$||F|| = \max \sum_{(j-1)} [f_{\bar{b}}|: i=1,N] \qquad (7)$$

As described in Ref.5 and the references therein.

VI. NEW POSSIBILITIES FOR CDIS INSTRUMENTS

The importance of any *a priori* knowledge of the object is well known[10]. The simulation step gives specific information about the absolute extent of the object field, points' size, and their distribution. Apart from any advantage this exact knowledge of the field will give to a given restoration scheme, and as an aid to accurately display unequally calibrated fields' restorations, a new possibility is the precise pixel-to-pixel addition and subtraction of outputs of separate instruments. When the two or more instruments have equal magnifications, and equivalent focusing and sensing capabilities, such as in an array of radio telescopes, such operations are straightforward. However if the separate instruments imaging the same object have different magnifications, aberrations, distortions and sensor or sampling irregularities, such addition or subtraction of the digital outputs becomes useless.

CDIS methods offer an elegant solution to this problem: if the two or more instruments are calibrated by identical simulation methods (simulating point size, intensity, orientation in space, etc.) then the columns of the resulting matrices F1, F2, F3...of the separate instruments will refer to the same points in space, and can simply be added up. A similar argument permits the addition (or subtraction, as the case may be) of the sensor rows of F, creating a composite F matrix that can be used to restore the combined S_j of the separate instruments. Alternately, the separate restored outputs of the different instruments can be combined after the separate computations are done. The results of a stable restoration will be without distortion in CDIS. So long as the PSFs have sufficient peaks to match the calibration point size, resulting in a stable F, the process of calibration will account for the severest distortions in PSF shape. This is so because of the absolute knowledge of the O_i positions, so object space can be referred to a fixed grid where restored points can be displayed, regardless of the distortions in the actual PSF. This aspect of CDIS can be useful in designing new types of imaging instruments using such hardware as crystals, gratings or 3-D

apertures of unknown transfer functions, or as a means to correct the distortions of more conventional instruments. A new kind of maging technique using unconventional â€˜instruments' such as a given geological formation refracting seismic signals, or reflecting optical or radar signals, will then become possible.

VII. AN EXPERIMENTAL RESTORATION USING CDIS METHODS

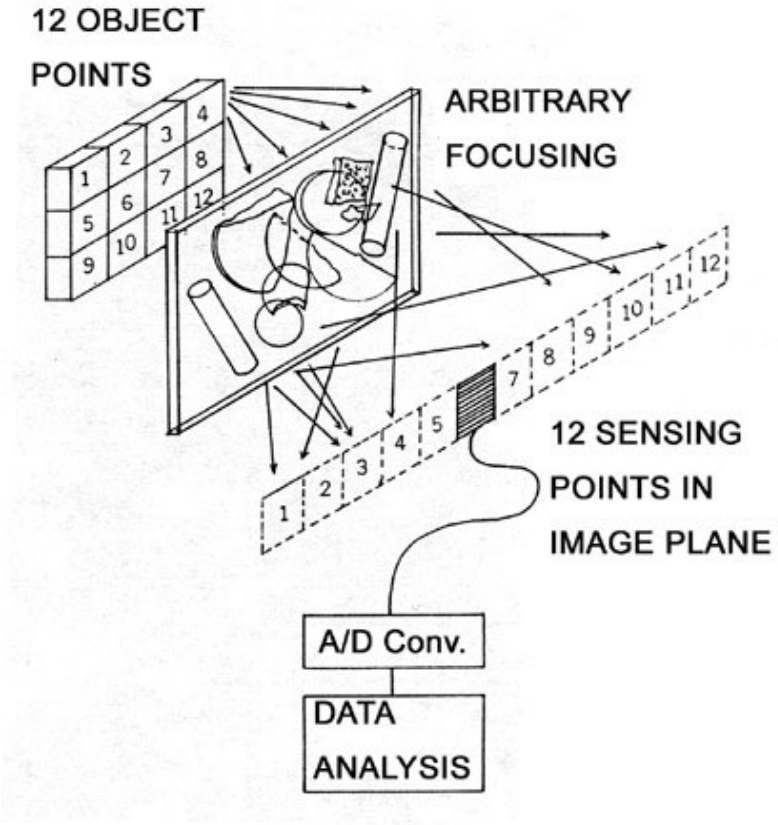

Fig. 6 Experimental set-up for CDIS imaging experiment. (a) 12 LED sources were used as calibration and object signals in turn. A sensor scanned 12 positions along an arbitrarily chosen straight path through the severely distorted overlapping images.

Fig. 6 shows the basic set-up used to test the CDIS premise that calibration permits imaging through unknown and even arbitrary hardware, which consisted in this case of a screen upon which was glued at random broken lenses and chunks of diffusing glass. O_i was a set of 12 light emitting diodes (LED) set near the screen, and giving a diffuse PSF shown in Fig 7a., while Fig. 7b. shows the direct image when several diodes are on simultaneously, to give some object pattern. The direct image from a pattern of, for example, 3 LEDs illuminated together becomes quite diffuse, because the already distorted individual PSFs are severely overlapped. A large detector sampled this image by scanning 12 sensing 'points' S_j along an arbitrarily chosen straight line through the image field. In other experiments the detector positions lay on a circle within the image plane, without affecting the successful restoration. Calibration consisted of switching on the first LED (O_1) and digitally storing the 12 detector readings S_1, S_2,..S_{12} as the first column f_{11},f_{12}..$f_{1\ 12}$ of an F matrix. Only the second LED (O_2) was then switched on and the second column's data was taken, and the process continued for all 12 LEDs until F was compiled.

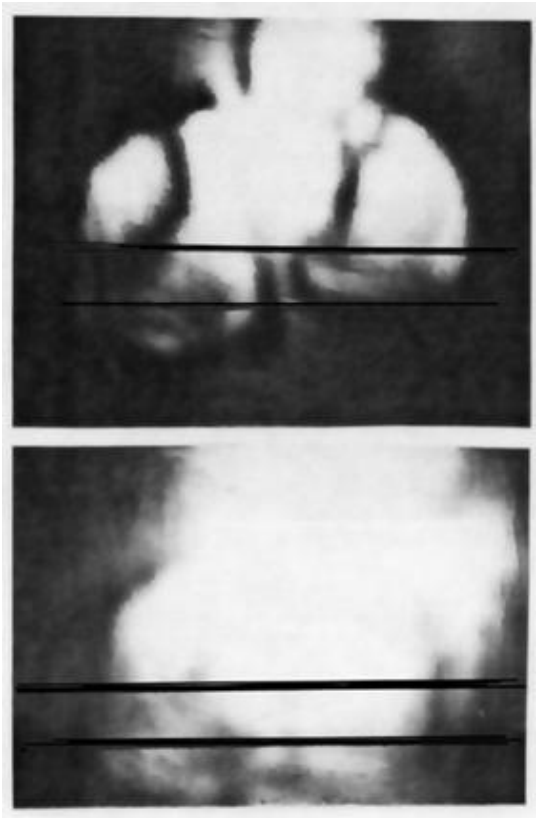

Fig. 7 (a,b). Aberrated images photographed from the setup of Fig.6. (a, top) Typical PSF from a single LED; the randomly chosen sampling path is shown by parallel lines. (b, bottom) Direct image of the 5 LEDs of pattern A of Fig. 9, showing severe superposition of 6 PSFs.

Fig.8 is a plot of the resulting SRF data of F, where each numbered curve indicates the particular column related to a numbered LED. It is interesting to note that no two curves are identical, and that for this coarse resolution the F matrix was well behaved, given the roughly 20dB signal to noise ratio (SNR) in the measurements. This F matrix thus represents an image field with total overlapping of all PSF. Imaging was performed with the same set of LEDs used for the calibration. In an actual instrument this is neither possible nor desirable. Fig.8 shows plots of three separate direct images S_j, A, B and C. Next to each curve is a small diagram showing the LED pattern that generated the image. Note that superposition of many PSFs has caused the S_j to have even less contrast than the SRF of Fig.7. In spite of that, a restoration was possible using the direct inverse, as in Eq. (5). Fig.10 plots the restored object for A, B, and C patterns of Fig.9. Note that all 'on' points are lower than the calibration intensity, 1, due to a dimming of all the LED set when more than one were switched on. Point 2 of pattern G is visibly lower than the rest, a filter having been put on that LED during imaging.

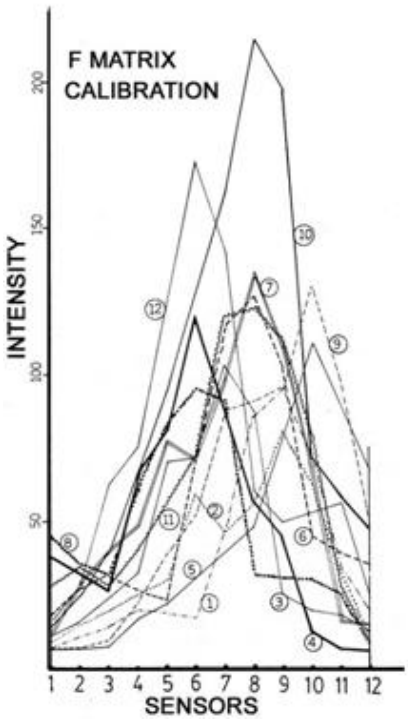

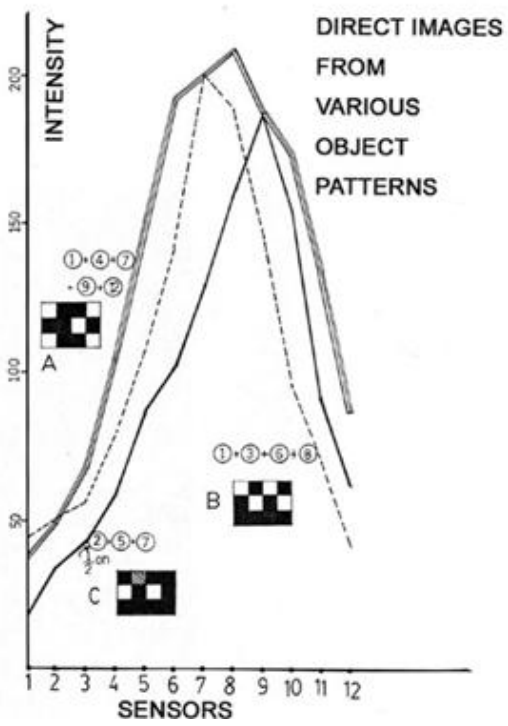

FIGURE 8 FIGURE 9

Fig. 8.(top,left) Graphs of the calibrated sensor data that form columns of the F matrix . Each of the 12 graphs shows the measured intensity plot of the image of a single object LED. They are the sensor response function (SRF), which is the PSF sampled from 12 sensor positions during calibration. Despite total superposition, each curve is significantly different from any other. See photo Fig.7(a)

Fig. 9.(top,right) The measured S_j outputs of three separate imaging situations from A, B and C object patterns, (shown in boxes adjoining the image plots). LED No.2 in pattern C was dimmed by a filter. See photo Fig.7(b) corresponding to the image of pattern A.

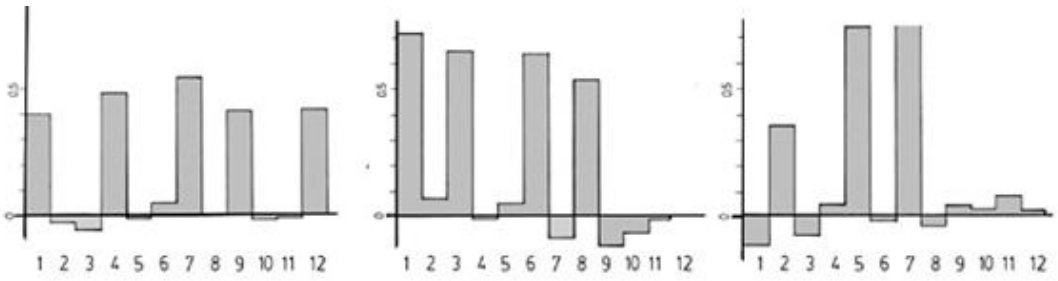

A B C

Fig. 10.Successfully restored object intensities computed with $O_i = F^{-1}.S_j$. The data of Fig. 8 was used to obtain the calibration matrix F. The sensor data S_j of the three test patterns A,B, and C of Fig. 9 was used in turn . The computed intensity of object 2 in C was correctly restored at half-strength because of the filter used over that particular LED.

Besides measurement noise there was considerable instability in the source. It was only possible to restore the image cast by a small number of objects due to the severe degradation due to the hardware: the PSFs were spread over many if not all of the sensors. In this case merely using smaller object and sensor size and calibrating more points will not increase the instrument's resolution, because the noise accumulated by one sensor tends to corrupt the restoration beyond a certain limit. With better focusing, a given sensor will receive signals from fewer object points and a finer calibration object and sensor size can be used. This will result in a higher signal-to-noise ratio (SNR) and a more sophisticated restoration scheme based on a large F becomes possible with greater resolution.

The process of point-by-point simulation to calibrate an instrument's impulse response has a curious historical antecedent. In the 10^{th} century, the Arab scientist Al-Hassan ibn al-Haytham (Alhazen) imaged several lamps lit singly and then together, through the pinhole of a camera obscura, noting that the image cast on the screen changed according to the number of lamps lit. This was to disprove an ancient belief that the eye emitted a sort of visual ray during vision. [18].

VIII. CONCLUSION

We have described a new imaging process, that of spatially calibrating an instrument's impulse response from chosen points in the object field, to obtain a discretized version of the transfer matrix of that instrument, including the peculiarities of the chosen object point size and distribution, and those of the set of sensors in the image field. Simple as it is, the resulting F matrix was shown to have useful applications to optimize existing restoration algorithms by giving a better algorithm-hardware fit. CDIS methods allow imaging through severely distorted systems, which can be used to design new types of instruments. Other possible uses for the F matrix are the accurate digital addition or subtraction of outputs from separate instruments, as a graphical or digital quality measure of an optical system, and as an aid in local restoration schemes using edge enhancement adjoining a dark field. The systems necessary to calibrate a particular instrument will vary, according to the type of signal, the required accuracy, size of aperture, and whether the signals simulated arrive from the near or far fields. The details of calibration methods are outside the scope of this introductory and general paper, but they need careful treatment.

IX. ACKNOWLEDGEMENTS

The idea that arbitrary PSFs can be simulated and calibrated was inspired by the published work of an artist, P. Hoenich [19] who created patterns out of the caustics of reflected sunlight off irregularly bent metal sheets. Mr. N. Asano kindly provided the sensor and related circuit. Thanks to the editor and referees of the Journal of the Optical Society of America, to Dr. J. Goodman and to Dr. P. Manly for helpful correspondence and advice.

- Vladimir Tamari invented the CDIS concept, designed and built the mechanical and optical experimental apparatus, wrote and illustrated this paper. Masato Kobori developed the necessary mathematical tools, assembled the sensing electronics for the collection of the experimental data, wrote and ran the BASIC program for the matrix inversions. The paper was submitted to the Journal of the Optical Society of America in April 1982 but was not published there. This digital version of the paper with minor revisions in the text and figures was made in July 2003.

REFERENCES

[1] G. Toraldo di Francia, "Capacity of an optical channel in the presence of noise", Opta Acta, 2 No.1 (1955).

[2] B.R. Frieden,"Maximum-information data processing: applications to optical signals", J.Opt.Soc.Am 71,294(1981).

3 C.E.Shannon & W. Weaver, The Mathematical Theory of Information U. Illinois Press (1949).

4 Born and Wolf Principles of Optics 6th. ed. p.482 Pergamon Press (1980)

5 M.J.Lahart, "Local image restoration by a least-squares method", J.Opt.Soc.Am. 69, 1333 (1979)

6 A.A. Sveshnikov, Problems in Probability Theory. Mathematical Statistics and the Theory of Random Functions.206, N.Y. (1968).

7 D.Burghes & A.Graham, Introduction to Control Theory including optimal control, p.3 .Ellis Horwood/John Wiley, N.Y. (1980).

8 M.Born & E.Wolf Principles of Optics, Pergamon Press 6th. ed. p.755 (1980).

9 O.N.Stavroudis, The Optics of Rays, Wavefronts and Caustics Academic Press, N.Y. p.276 (1972)

10 B.R. Frieden,"Image Enhancement and Restoration" in Picture Processing and Digital Filtering, T.S.Huang, Ed. Springer-Verlag, Berlin -Heidleberg.N.Y. (1975).

11 R.W. Gerchberg. Opta Acta 21,709 (1974).

12 G.W. Helstrom "Image restoration by the method of least squares", J.Opt. Soc. Am. 57, 297 (1967).

13 R.M. Mammone & G.Eichmann "Super-resolving image restoration using linear programming", Appl. Opt. 21, 496 (1982).

14 K.Murata, "Instruments for measuring the Optical Transfer Function", Progress in Optics. E.Wolf,Ed. North-Holland(1966).

15 J. W. Goodman, A. R. Dias, and L. M. Woody, \Fully parallel, high-speed incoherent

optical method for performing discrete Fourier transforms," Opt. Lett. 2, 1-3

(January 1978).

16 E.Fenimore & G.Weston "Fast delta Hadamard transform" Appl. Opt. 20,3058 (1981)

17 D.S.Goodman "Graphical Method for Image Irradiance Determination" (A), J.Opt.Soc.Am. 71,1626 (l98l).

18 H. ibn al-Haytham Kitab al-Manazir Cairo llth.c.in Arabic.Latin translation Opticae Thesaurus, Alhazen Arabis libri septem nuncprimum editi Basle (1572).

19 P.Hoenich "Light Symphony, No.1: A Kinetic Pictorial Artwork with Light" Leonardo,14 No.1,p.38 Pergamon Press (l98l).